# Covalent Three-Dimensional Titanium(IV)−Aryloxide Networks

**ARTICLE** *in* INORGANIC CHEMISTRY · AUGUST 1999

Impact Factor: 4.76 · DOI: 10.1021/ic990109b · Source: PubMed

# Covalent Three-Dimensional Titanium(IV)−Aryloxide Networks

**Thomas P. Vaid, Joseph M. Tanski, John M. Pette, Emil B. Lobkovsky, and Peter T. Wolczanski***

Cornell University, Baker Laboratory, Department of Chemistry & Chemical Biology, Ithaca, New York 14853

*Received January 25, 1999*

$Ti(^iOPr)_4$ was treated with 2.58 equiv of hydroquinone in THF to yield a red-orange powder formulated as $[Ti(OC_6H_4O)_a(OC_6H_4OH)_{3.34-1.83a}(O^iPr)_{0.66-0.17a}(THF)_{0.2}]_n$ (**1**, $(0.91 \le a \le 1.82)$) based upon $D_2O$/DCl quenching studies. Treatment of **1** with an excess of hydroquinone in $Et_2O$ or DME afforded burgundy $[Ti_2(\mu_{1,4}\text{-}OC_6H_4O)_2(\mu_{1,4}\text{-}OC_6H_4OH)_2(\mu\text{-}OC_6H_4OH)_2]_\infty$ (**2**). Burgundy $[Ti_2(\mu_{1,4}\text{-}OC_6H_4O)_2(\mu_{1,4}\text{:}\eta^2,\eta^1\text{-}OC_6H_4O)_2(OH_2)_2\cdot(H_2O)_2\cdot(HOC_6H_4OH)\cdot(MeCN)]_\infty$ (**4**) was prepared from **1** and excess wet hydroquinone in $CH_3CN$. The acetonitrile in **4** can be exchanged for THF or DME. Treatment of $Ti(O^iPr)_4$ with ∼4 equiv of 2,7-dihydroxynaphthalene in $Et_2O$ at 100 °C (2 days) in a sealed tube yielded orange crystals of $[Ti_2(\mu_{1,7}\text{-}OC_{10}H_6O)_2(\mu_{1,7}\text{:}\eta^2,\eta^1\text{-}OC_{10}H_6OH)_2(O^iPr)_2]_\infty$ (**5**). Diffraction studies were conducted at the Cornell High Energy Synchrotron Source (CHESS) because of the small crystal sizes. **2** ($C_{18}H_{14}O_6Ti$, monoclinic, $P2_1/n$, $a = 9.624$ (2), $b = 11.283$ (2), $c = 14.916$ (3), $\beta = 90.47(3)°$, $Z = 4$), **4** ($C_{32}H_{33}NO_{14}Ti_2$, monoclinic, $P2_1/n$, $a = 16.137$ (3), $b = 10.762$ (2), $c = 20.368$ (4), $\beta = 111.65(3)°$, $Z = 4$), and **5** ($C_{23}H_{20}O_5Ti$, orthorhombic, *Pbca*, $a = 11.095$ (2), $b = 17.970$ (4), $c = 19.484$ (4), $Z = 8$) are 3-dimensional materials based on diaryloxide connectivity between geometrically similar edge shared (i.e., $Ti_2(\mu\text{-}OAr)_2$) bioctahedral dititanium building blocks. While **2** and **5** possess a roughly body-centered arrangement of dititanium units, **4** has a hexagonal secondary structural motif. The nature of crystallization through alcoholysis is also discussed.

## Introduction

Under the guise of crystal engineering,[1,2] the investigation of coordination polymerization has undergone a recent burst of activity.[3,4] The utilization of organic components, primarily rigid, di- or trifunctionalized ligands, in concert with metals of known coordination tendencies, has permitted some control of the coordination geometry based on stoichiometry.[5] This contrasts greatly with the synthesis of natural or more traditional inorganic solid-state compounds, where limited predictive capacity exists.

Many structurally intriguing 2- and 3-dimensional metal−organic coordination compounds have been discovered. While early versions typically used main group or transition metals best construed as charged, spherical components (e.g., $Ag^+$,[6−9] $Cd^{2+}$, $Zn^{2+}$,[10] and Cu(I)[11,12]) at their cores, a greater variety of transition metals—even metal oxides[13]—are now incorporated into matrixes typically defined by aryl carboxylates,[14,15] nitriles,[16,17] oxalates,[18,19] pyridines,[20−25] pyrazines, and various

(1) Schmidt, G. M. J. *Pure Appl. Chem.* **1971**, *27*, 647−679.
(2) Desiraju, G. R. *Angew. Chem., Int. Ed. Engl.* **1995**, *34*, 2311−2327.
(3) Robson, R. In *Comprehensive Supramolecular Chemistry*; Atwood, J. L., Davies, J. E. D., MacNicol, D. D., Vögtle, F., Toda, F., Bishop, R., Eds.; Pergamon: Oxford, 1996; Vol. 6, pp 733−755.
(4) Batten, S. R.; Robson, R. *Angew. Chem., Int. Ed. Engl.* **1998**, *37*, 1460−1494.
(5) For recent comments on intrisic structural problems, see: Zaworotko, M. J. *Angew. Chem., Int. Ed.* **1998**, *37*, 1211−1213.
(6) (a) Abrahams, B. F.; Jackson, P. A.; Robson, R. *Angew. Chem., Int. Ed.* **1998**, *37*, 2656−2659. (b) Hoskins, B. F.; Robson, R.; Slizys, D. A. *J. Am. Chem. Soc.* **1997**, *119*, 2952−2953.
(7) Carlucci, L.; Ciani, G.; Proserpio, D. M.; Sironi, A. *Inorg. Chem.* **1998**, *37*, 5941−5943.
(8) Hirsch, K. A.; Wilson, S. R.; Moore, J. S. *J. Chem. Soc., Chem. Commun.* **1998**, 13−14.
(9) Blake, A. J.; Champness, N. R.; Chung, S. S. M.; Li, W.-S.; Schröder, M. *J. Chem. Soc., Chem. Commun.* **1997**, 1675−76.
(10) Lin, W.; Evans, O. R.; Xiong, R.-G.; Wang, Z. *J. Am. Chem. Soc.* **1998**, *120*, 13272−13273.
(11) Young, D. M.; Geiser, U.; Schultz, A. J.; Wang, H. H. *J. Am. Chem. Soc.* **1998**, *120*, 1331−1332.
(12) Kuroda-Sowa, T.; Horino, T.; Yamamoto, M.; Ohno, Y.; Maekawa, M.; Munakata, M. *Inorg. Chem.* **1997**, *36*, 6382−6389.
(13) (a) Hagrman, D.; Zubieta, J. *J. Chem. Soc., Chem. Commun.* **1998**, 2005−2006. (b) Hagrman, D.; Sangregorio, C.; O'Connor, C. J.; Zubieta, J. *J. Chem. Soc., Dalton Trans.* **1998**, 3707−3709. (c) Hagrman, D.; Haushalter, R. C.; Zubieta, J. *Chem. Mater.* **1998**, *10*, 361−365. (d) Zapf, P. J.; Warren, C. J.; Haushalter, R. C.; Zubieta, J. *J. Chem. Soc., Chem. Commun.* **1997**, 1543−1544.
(14) (a) Yaghi, O. M.; Davis, C. E.; Li, G.; Li, H. *J. Am. Chem. Soc.* **1997**, *119*, 2861−2868. (b) Yaghi, O. M.; Li, H.; Groy, T. L. *J. Am. Chem. Soc.* **1996**, *118*, 9096−9101.
(15) Kepert, C. J.; Rosseinsky, M. J. *J. Chem. Soc., Chem. Commun.* **1998**, 31−32.
(16) (a) Gardner, G. B.; Kiang, Y.-H.; Lee, S.; Asgaonkar, A.; Vendataraman, D. *J. Am. Chem. Soc.* **1996**, *118*, 6946−6953. (b) Gardner, G. B.; Venkataraman, D.; Moore, J. S.; Lee, S. *Nature* **1995**, *374*, 792−795.
(17) (a) Batten, S. R.; Hoskins, B. F.; Robson, R. *Inorg. Chem.* **1998**, *37*, 3432−3435. (b) Batten, S. R.; Jensen, P.; Moubaraki, B.; Murray, K. S.; Robson, R. *J. Chem. Soc., Chem. Commun.* **1998**, 439−440.
(18) (a) Pellaux, R.; Schmalle, H. W.; Huber, R.; Fischer, P.; Hauss, T.; Ouladdiaf, B.; Decurtins, S. *Inorg. Chem.* **1997**, *36*, 2301−2308. (b) Decurtins, S.; Schmalle, H. W.; Schneuwly, P.; Ensling, J.; Gütlich, P. *J. Am. Chem. Soc.* **1994**, *116*, 9521−9528.
(19) Clemente-Léon, M.; Coronado, E.; Galán-Mascarós, J.-R.; Gómez-Garcia, C. J. *J. Chem. Soc., Chem. Commun.* **1997**, 1727−28.
(20) Carlucci, L.; Ciani, G.; Macchi, P.; Proserpio, D. M. *J. Chem. Soc., Chem. Commun.* **1998**, 1837−1838.
(21) Power, K. N.; Hennigar, T. L.; Zaworotko, M. J. *J. Chem. Soc., Chem. Commun.* **1998**, 595−596.
(22) Hagrman, D.; Hammond, R. P.; Haushalter, R.; Zubieta, J. *Inorg. Chem.* **1971**, *10*, 2091−2100.
(23) Hong, C. S.; Do, Y. *Inorg. Chem.* **1998**, *37*, 4470−4472.
(24) MacGillivray, L. R.; Groeneman, R. H.; Atwood, J. L. *J. Am. Chem. Soc.* **1998**, *120*, 2676−2677.
(25) Yaghi, O. M.; Li, H.; Groy, T. L. *Inorg. Chem.* **1997**, *36*, 4292−4293.

10.1021/ic990109b CCC: $18.00 
Published on Web 06/23/1999

other appropriately functionalized organic spacers.[26−36] Most importantly, several transition metal compounds exhibit intriguing magnetic properties,[17,18,23,30,37] especially those containing cyanide bridges,[38−43] while other materials display some unusual inclusion reactivity[44−51] and catalysis.[52,53]

In this article, the synthesis and characterization of covalent, metal−organic networks (CMON) based on titanium−aryloxide bonds is described. Unlike most coordination polymers, the construction of these networks cannot be accomplished via reversible dative bonding, but arises through a chemical reaction—the alcoholysis of a precursor titanium alkoxide. The linkages thus formed are strong, covalent bonds that are distinct from typical dative interactions[54] which characterize virtually every other metal−organic network.[55] The initial synthetic and structural forays into this new class of solid-state materials are reported below; a preliminary account of one derivative has appeared.[56]

## Results

**Syntheses. 1. Precursor Preparation.** In 1990, Burch reported the synthesis of an amorphous titanium quinone material produced upon alcoholysis—with hydroquinone—of $Ti(NMe_2)_4$.[57] Consider this procedure as a modified sol−gel method, whereby the two hydroxyl functionalities of the organic molecule react with the amides to eliminate 2 $HNMe_2$, thereby spanning two metal centers just as water would lead to $\mu$-oxide formation. Initially, a related amorphous material was used as a precursor to crystalline, covalent titanium quinone networks, but subsequent studies have shown that the materials may be directly synthesized, albeit with the occasional incorporation of ligands originating from the source of Ti(IV).

Using a modified procedure of Burch,[57] $Ti(^iOPr)_4$ was treated with 2.58 equiv of hydroquinone in THF to yield a red-orange powder upon drying. The free-flowing powder was formulated as $[Ti(OC_6H_4O)_a(OC_6H_4OH)_{3.34-1.83a}(O^iPr)_{0.66-0.17a}(THF)_{0.2}]_n$ (**1**, eq 1) based upon quenching studies. Exposure of **1** to $D_2O$/DCl afforded a $DOC_6H_4OD/DO^iPr$/THF mixture whose ratio could be determined via integration of the $^1H$ NMR spectrum. Note that this reaction does not distinguish between a quinone (i.e., $Ti-OC_6H_4O-Ti$) linkage, semiquinone (i.e., $Ti-OC_6H_4OH$) functionality, or hydroquinone, hence certain assumptions and some interpretation of the integrated ratio is necessary. For example, in eq 1 the titanium was assumed to remain Ti(IV), yielding a range of values of semiquinone and $O^iPr$ that are possible. The stoichiometry indicated in eq 1 was empirically determined to yield the best and most reproducible material, which was shown to be amorphous by powder XRD.

$$Ti(^iOPr)_4 + 2.58\ HOC_6H_4OH \xrightarrow{\text{THF, 25 °C}} {}^1/_n[Ti(OC_6H_4O)_a(OC_6H_4OH)_{3.34-1.83a}(O^iPr)_{0.66-0.17a}(THF)_{0.2}]_n \quad \mathbf{1}\ (0.91 \le a \le 1.82) + (3.34 + 0.17a)HO^iPr \quad (1)$$

When isopropoxide was suspected as interfering in the crystallization processes, use of **1** minimized the possibility of $O^iPr$ incorporation into the product. In comparison to direct materials synthesis from $Ti(O^iPr)_4$, the synthesis of **1** adds an additional step, yet often decreases the time of sample preparation in subsequent steps because it is a readily handled solid.

**2. Precursor-Derived CMON Materials.** Treatment of precursor **1** with an excess of hydroquinone (typically ∼10−20 equiv) in $Et_2O$ or DME afforded burgundy, microcrystalline $[Ti_2(\mu_{1,4}\text{-}OC_6H_4O)_2(\mu_{1,4}\text{-}OC_6H_4OH)_2(\mu\text{-}OC_6H_4OH)_2]_\infty$ (**2**). Quenching ($D_2O$/DCl) studies confirmed the presence of hydroquinone when ether was the solvent (occasional traces of ether were observed), but in DME, significant, yet spurious amounts of the solvent were also noted. Since the powder XRD patterns of material produced in either solvent were identical, and the absence of solvent was confirmed by a single-crystal XRD experiment, the source of the DME remains unknown. It is possible that cavities in the material (vide infra) may be large enough to trap some solvent, but it is more likely that crystal

$$\mathbf{1} \xrightarrow[\substack{Et_2O \text{ or DME,}\\ \sim 1\ M\ HOC_6H_4OH}]{\text{100 °C, 1−4 days}} \underset{\mathbf{2}}{[Ti_2(\mu_{1,4}\text{-}OC_6H_4O)_2(\mu_{1,4}\text{-}OC_6H_4OH)_2(\mu\text{-}OC_6H_4OH)_2]_\infty} \quad (2)$$


(26) Lloret, F.; De Munno, G.; Julve, M.; Cano, J.; Ruiz, R.; Caneschi, A. *Angew. Chem., Int. Ed.* **1998**, *37*, 135−138.
(27) Tong, M. L.; Chen. X.-M.; Yu, X.-L. *J. Chem. Soc., Dalton Trans.* **1998**, 5−6.
(28) Neels, A.; Neels, B. M.; Stoeckli-Evans, H.; Clearfield, A.; Poojary, D. M. *Inorg. Chem.* **1997**, *36*, 3402−3409.
(29) Carlucci, L.; Ciani, G.; Proserpio, D. M.; Sironi, A. *Inorg. Chem.* **1995**, *34*, 5698−5700.
(30) de Muro, I. G.; Mautner, F. A.; Insausti, M.; Lezama, L.; Arriortua, M. I.; Rojo, T. *Inorg. Chem.* **1998**, *37*, 3243−3251.
(31) Rettig, S. J.; Storr, A.; Summers, D. A.; Thompson, R. C.; Trotter, J. *J. Am. Chem. Soc.* **1997**, *119*, 8675−8680.
(32) Chesnut, D. J.; Zubieta, J. *J. Chem. Soc., Chem. Commun.* **1998**, 1707−1708.
(33) Knoeppel, D. W.; Liu, J.; Meyers, E. A.; Shore, S. G. *Inorg. Chem.* **1998**, *37*, 4828−4837.
(34) Atherton, Z.; Goodgame, D. M. L.; Menzer, S.; Williams, D. J. *Inorg. Chem.* **1998**, *37*, 849−858.
(35) Wu, H.-P.; Janiak, C.; Uehlin, L.; Klüfers, P.; Mayer, P. *J. Chem. Soc., Chem. Commun.* **1998**, 2637−2638.
(36) Blake, A. J.; Champness, N. R.; Crew, M.; Hanton, L. R.; Parsons, S.; Schröder, M. *J. Chem. Soc., Dalton Trans.* **1998**, 1533−1534.
(37) (a) Manson, J. L.; Campana, C.; Miller, J. S. *J. Chem. Soc., Chem. Commun.* **1998**, 251−252. (b) Manson, J. L.; Incarvito, C. D.; Rheingold, A. L.; Miller, J. S. *J. Chem. Soc., Dalton Trans.* **1998**, 3705−3706.
(38) Entley, W. R.; Girolami, G. S. *Science* **1995**, *268*, 397−400.
(39) (a) Ferlay, S.; Mallah, T.; Ouahés, R.; Veillet, P.; Verdaguer, M. *Nature* **1995**, *378*, 701−706. (b) Mallah, T.; Thiebaut, S.; Verdaguer, M.; Veillet, *Science* **1993**, *262*, 1554−1564.
(40) Larionova, J.; Clerac, R.; Sanchiz, J.; Kahn, O.; Golhen, S.; Ouahab, L. *J. Am. Chem. Soc.* **1998**, *120*, 13088−13095.
(41) Miyasaka, H.; Okawa, H.; Miyazaki, A.; Enoki, T. *Inorg. Chem.* **1998**, *37*, 4878−4883.
(42) (a) Fukita, N.; Ohba, M.; Okawa, H.; Matsuda, K.; Iwamura, H. *Inorg. Chem.* **1998**, *37*, 842−848. (b) Ohba, M.; Fukita, M.; Okawa, H. *J. Am. Chem. Soc.* **1997**, *119*, 1011−1019.
(43) Manson, J. L.; Buschmann, W. E.; Miller, J. S. *Angew. Chem., Int. Ed.* **1998**, *37*, 783−784.
(44) Janiak, C. *Angew. Chem., Int. Ed. Engl.* **1997**, *36*, 1431−1434.
(45) Li, H.; Eddaoudi, M.; Groy, T. L.; Yaghi, O. M. *J. Am. Chem. Soc.* **1998**, *120*, 8571−8572.
(46) Subramanian, S.; Zaworotko, M. J. *Angew. Chem., Int. Ed. Engl.* **1995**, *34*, 2127−2129.
(47) Kondo, M.; Yoshitomi, T.; Seki, K.; Matsuzaka, H.; Kitagawa, S. *Angew. Chem., Int. Ed. Engl.* **1997**, *36*, 1725−1727.
(48) Brandt, P.; Brimah, A. K.; Fischer, R. D. *Angew. Chem., Int. Ed. Engl.* **1988**, *27*, 1521−1522.
(49) Groeneman, R. H.; MacGillivray, L. R.; Atwood, J. L. *J. Chem. Soc. Chem. Commun.* **1998**, 2736−2736.
(50) Ruiz, E.; Alvarez, S. *Inorg. Chem.* **1995**, *34*, 3260−3269.
(51) Abrahams, B. F.; Hardy, M. J.; Hoskins, B. F.; Robson, R.; Williams, G. A. *J. Am. Chem. Soc.* **1992**, *114*, 10641−10643.
(52) Fujita, M.; Kwon, Y. J.; Washizu, S.; Ogura, K. *J. Am. Chem. Soc.* **1994**, *116*, 1151−1152.
(53) Sawaki, T.; Dewa, T.; Aoyama, Y. *J. Am. Chem. Soc.* **1998**, *120*, 8539−8540.
(54) Haaland, A. *Angew. Chem., Int. Ed. Engl.* **1989**, *28*, 992−1007.
(55) For another example of a network containing titanium, see: Liu, F.-Q.; Tilley, T. D. *J. Chem. Soc., Chem. Commun.* **1998**, 103−104.
(56) Vaid, T. P.; Lobkovsky, E. B.; Wolczanski, P. T. *J. Am. Chem. Soc.* **1997**, *119*, 8742−8743.
(57) Burch, R. R. *Chem. Mater.* **1990**, *2*, 633−635.

imperfections include pits where solvent is occluded. Visually (light microscope), **2** appeared to be produced in quantitative yield, and a powder XRD generated from single-crystal data matched that obtained from the bulk.

The combination of **1**, hydroquinone, and a relatively weak donor solvent was not limited to $Et_2O$ and DME, but efforts to obtain sufficiently large crystals from THF, EtCN, PhCN, and dimethoxymethane failed. Other solvents resulted in material of little or no visible (light microscope, powder XRD) crystallinity. As an example, consider the case of THF, shown in eq 3. Standard quenching procedures ($D_2O$/DCl; integration of

$$\mathbf{1} \xrightarrow[\text{THF, } \sim 1\text{ M } HOC_6H_4OH]{100\ ^\circ\text{C, 2 days}} [Ti(OC_6H_4O)_{2-a}(OC_6H_4OH)_{2a}(THF)_{0.20(2+a)}]_\infty \quad (3)$$
$$\mathbf{3}$$

hydroquinone aromatic protons relative to THF resonances) suggested that the THF content—relative to hydroquinone—of $[Ti(OC_6H_4O)_{2-a}(OC_6H_4OH)_{2a}(THF)_{0.20(2+a)}]_\infty$ (**3**) was dependent on the specific experiment, yet its lattice was clearly different than **2** by powder XRD. Visual inspection by light microscopy revealed the presence of agglomerate crystals, with some rectangular shaped individuals; unfortunately their size—typically $4 \times 10$ $\mu$m on a side—precluded single-crystal analysis. This case is representative of the majority of synthetic forays into this class of network compounds.

Initial sets of experiments were conducted with commercial hydroquinone that was not subsequently purified. Since no water incorporation was noted in material prepared from a variety of dried solvents (e.g., $Et_2O$, DME, and THF), the network prepared in acetonitrile was a surprise. The compound, prepared similarly to **2**, was determined to be burgundy, microcrystalline $[Ti_2(\mu_{1,4}\text{-}OC_6H_4O)_2(\mu_{1,4}{:}\eta^2,\eta^1\text{-}OC_6H_4O)_2(OH_2)_2{\cdot}(H_2O)_2{\cdot}(HOC_6H_4OH){\cdot}(MeCN)]_\infty$ (**4**) according to a single-crystal XRD experiment, although quenching studies indicated a 5:2 ratio of hydroquinone to acetonitrile, implying $x = 2$ in eq 4, in

$$\mathbf{1} \xrightarrow[\sim 1\text{ M } HOC_6H_4OH]{100\ ^\circ\text{C, 2 days, } CH_3CN,} [Ti_2(\mu_{1,4}\text{-}OC_6H_4O)_2(\mu_{1,4}{:}\eta^2,\eta^1\text{-}OC_6H_4O)_2(OH_2)_2{\cdot}(H_2O)_2{\cdot}(HOC_6H_4OH){\cdot}x(MeCN)]_\infty \quad (4)$$
$$\mathbf{4}\ (x = 1 \text{ or } 2)$$

agreement with elemental analysis. It is quite conceivable that additional $CH_3CN$ is disordered in cavities of **4**, which are demonstrably larger than those of **2**. However, a difference Fourier map from the crystal structure (vide infra) had a largest difference peak of 0.493 electron/Å$^3$, implying that it was unlikely that additional heavy atoms were present. When the commercial hydroquinone—assayed and shown to contain water by $^1$H NMR spectroscopy—was dried and recrystallized, compound **4** could not be prepared by the route indicated in eq 4, ruling out the solvent or degradation (e.g., water loss from $^i$PrO fragments) as possible sources of the $H_2O$. When water was subsequently added to the "dry" reaction mixture, **4** was synthesized.

In an attempt to convert **4** to the structure of the compound produced in THF (**3**), **4** was heated to 100 °C in a THF—hydroquinone solution. Instead, powder XRD showed that the unit cell of **4** was maintained, while $^1$H NMR spectroscopy revealed that the acetonitrile had been exchanged for THF. A similar exchange occurred in DME, indicating that the titanium—quinone lattice was maintained as its lattice solvent was exchanged. Any water exchange could not be confidently assayed due to the nature of the quenching studies.

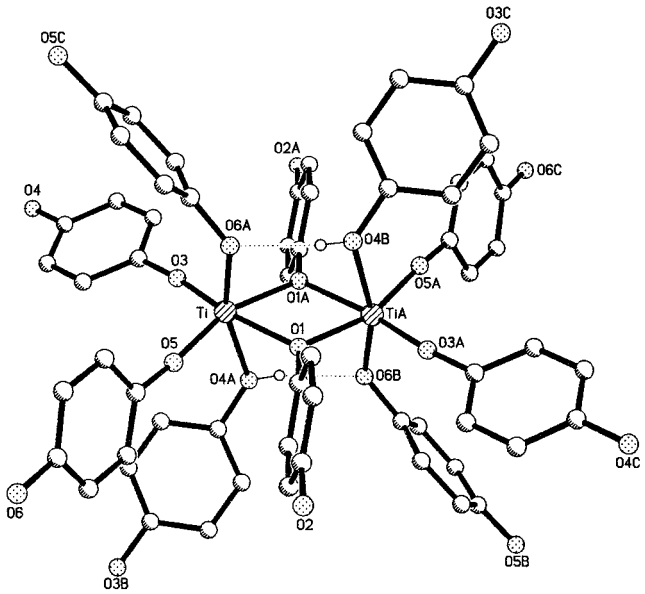


**Figure 1.** Bioctahedral dititanium building block of $[Ti_2(\mu_{1,4}\text{-}OC_6H_4O)_2(\mu_{1,4}\text{-}OC_6H_4OH)_2(\mu\text{-}OC_6H_4OH)_2]_\infty$ (**2**).

**3. Direct Synthesis of CMON Materials.** After the above experiments, it was determined that under the correct conditions, direct synthesis from $Ti(O^iPr)_4$, excess hydroquinone and the appropriate solvent would yield a majority of the materials previously discovered via alcoholysis of **1**. While this method permits expansion of the number of variables—principally organic spacers—in the synthesis of CMON materials without the need for preparing different precursor powders, it is not without the occasional pitfall.

Treatment of $Ti(O^iPr)_4$ with ~4 equiv of 2,7-dihydroxynaphthalene in $Et_2O$ at 100 °C in a sealed tube yielded visible orange crystals of $[Ti_2(\mu_{1,7}\text{-}OC_{10}H_6O)_2(\mu_{1,7}{:}\eta^2,\eta^1\text{-}OC_{10}H_6OH)_2(O^iPr)_2]_\infty$ (**5**) after 2 days (eq 5), and crystals amenable to single-crystal

$$Ti(O^iPr)_4 + \text{excess } 2,7\text{-}(OH)_2C_{10}H_6 \xrightarrow{Et_2O,\ 100\ ^\circ\text{C, } \sim 2\text{ days}} [Ti_2(\mu_{1,7}\text{-}OC_{10}H_6O)_2(\mu_{1,7}{:}\eta^2,\eta^1\text{-}OC_{10}H_6OH)_2(O^iPr)_2]_\infty \quad (5)$$
$$\mathbf{5}$$

X-ray analysis after 30 days. A $D_2O$/DCl quench of the material revealed 2,7-$(OD)_2C_{10}H_6$:$DO^iPr \sim 2{:}1$, implicating retention of some isopropoxide or 2-propanol units. While a series of dihydroxy aromatics (e.g., 1,3-$(OH)_2C_6H_4$, various dihydroxy naphthalenes) were applied in a manner similar to eq 5, and some yielded crystalline material from nondonor solvents, at this time only the 2,7-dihydroxynaphthalene derivative has proven to be structurally characterizable.

**X-ray Structural Studies. 1. General Aspects.** Single-crystal sizes of samples of **2**, **4** and **5** precluded analysis by the conventional X-ray equipment available, hence diffraction studies were conducted at the Cornell High Energy Synchrotron Source (CHESS, Table 1). The crystals were invariably asymmetric, such that each had at least one side $<20$ $\mu$m, and in no case was a data-to-parameter ratio of 10 obtained; in one case (**5**), only an isotropic refinement was reasonable. Despite these and other difficulties related to crystal size, satisfactory structures were obtained, in part because the rigid groups used in constructing the networks minimize disorder problems. The networks are quite dense, ranging from 1.45 g/cm$^3$ in **5** to 1.52

**Table 1.** X-ray Crystallographic Data on CMON Derivatives (Crystal Data, Data Collection, and Refinement)

| | **2** | **4** | **5** |
|---|---|---|---|
| cryst size, $\mu$m | 60 × 20 × 20 | 40 × 40 × 5 | 90 × 70 × 10 |
| empirical formula | $C_{18}H_{14}O_6Ti$ | $C_{32}H_{33}NO_{14}Ti_2$ | $C_{23}H_{20}O_5Ti$ |
| fw | 374.19 | 751.39 | 424.29 |
| space group | $P2_1/n$ | $P2_1/n$ | $Pbca$ |
| $a$, Å | 9.624 (2) | 16.137 (3) | 11.095 (2) |
| $b$, Å | 11.283 (2) | 10.762 (2) | 17.970 (4) |
| $c$, Å | 14.916 (3) | 20.368 (4) | 19.484 (4) |
| $\beta$, deg | 90.47 (3) | 111.65 (3) | 90 |
| $V$, Å$^3$ | 1619.6 (5) | 3287.7 (11) | 3884.7 (13) |
| $Z$ | 4 | 4 | 8 |
| $\rho_{calcd}$, g cm$^{-3}$ | 1.535 | 1.518 | 1.451 |
| $\mu$, mm$^{-1}$ | 0.561 | 0.558 | 0.474 |
| $T$ (K) | 110 (2) | 113 (2) | 108 (2) |
| $\lambda$ (Å) | 0.98000 Å (synchrotron) | 0.98000 Å (synchrotron) | 0.90800 Å (synchrotron) |
| no. of reflcns collctd | 1451 | 2721 | 1809 |
| no. of indepdt reflcns/restr/params | 1451/0/227 | 2721/0/446 | 1809/0/122 |
| *GOF* on $F^2$ [a] | 1.061 | 1.024 | 2.533 |
| $R$ indicies [$I > 2s(I)$][b] | $R_1 = 0.0688$, w$R_2 = 0.1942$ | $R_1 = 0.1125$, w$R_2 = 0.3023$ | $R_1 = 0.0842$, w$R_2 = 0.2308$ |
| $R$ indicies (all data)[b] | $R_1 = 0.0751$, w$R_2 = 0.2280$ | $R_1 = 0.1304$, w$R_2 = 0.3225$ | $R_1 = 0.0937$, w$R_2 = 0.2733$ |

[a] $GOF = [\sum w(|F_o| - |F_c|)^2/(n-p)]^{1/2}$, $n$ = number of independent reflections, $p$ = number of parameters. [b] $R_1 = \sum||F_o| - |F_c||/\sum|F_o|$; w$R_2 = [\sum w(|F_o| - |F_c|)^2/\sum \omega F_o^2]^{1/2}$.

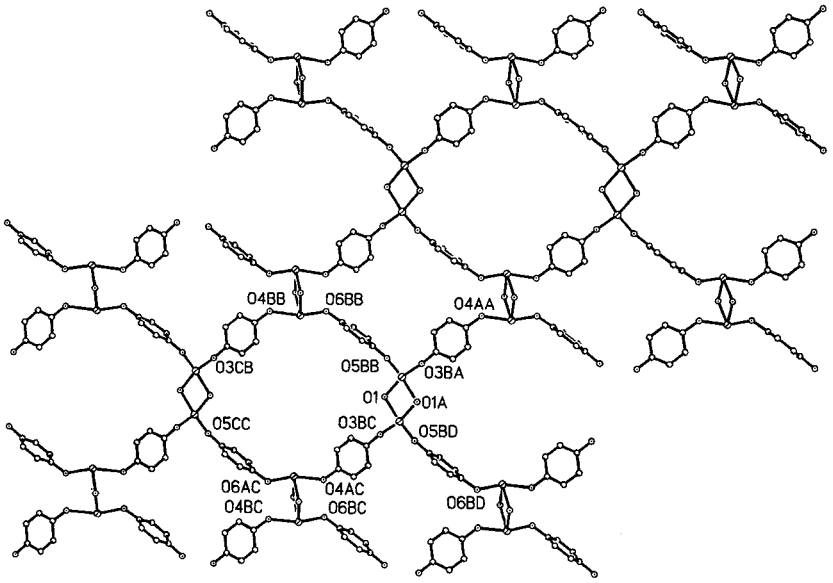


**Figure 2.** One of the two nets showing the axial (O4, O6) to equatorial (O3, O5) connectivity of $[Ti_2(\mu_{1,4}\text{-}OC_6H_4O)_2(\mu_{1,4}\text{-}OC_6H_4OH)_2(\mu\text{-}OC_6H_4\text{-}OH)_2]_\infty$ (**2**); the $\mu$-$OC_6H_4OH$ bridges have been removed for clarity.

and 1.54 g/cm$^3$ in **4** and **2**, and have similar light atom (i.e., C/N/O) to Ti ratios (23.5−25). To achieve this density, the larger cavities of **4** are filled with $H_2O$, hydroquinone, and acetonitrile molecules. Perhaps the slightly lower density in **5** reflects the difficulties in efficiently packing the larger naphthalene units in comparison to a benzene fragment.

**2. $[Ti_2(\mu_{1,4}\text{-}OC_6H_4O)_2(\mu_{1,4}\text{-}OC_6H_4OH)_2(\mu\text{-}OC_6H_4OH)_2]_\infty$ (2).** The 3-dimensional network of **2** stems from four 1,4-diphenoxide and four 4-hydroxyphenoxide connections linking roughly bioctahedral dititanium units. The geometry of the dititanium unit is reminiscent of $[(PhO)_3(PhOH)Ti]_2(\mu\text{-}OPh)_2$,[58] and the related $[(PhO)Cl_2Ti]_2(\mu\text{-}OPh)_2$.[59] Figure 1 shows this building block, replete with its connecting branches and two 4-hydroxyphenoxide bridging groups. Consider the equatorial plane to contain 4-hydroxyphenoxide bridges ($d$(Ti−O) = 2.042, 2.047 Å) that acutely span the titaniums (∠O1−Ti−O1A = 73.5(2)°, ∠Ti−O−Ti = 106.5(2)°), and two other relatively linear (∠Ti−O3−C7 = 173.0(3)°, ∠Ti−O5−C13 = 164.1(3)°) aryloxide linkages ($d$(Ti−O3) = 1.782(3) Å, $d$(Ti−O5) = 1.794(4) Å) that have an obtuse relationship (∠O3−Ti−O5 = 99.8(2)°). In the axial positions, a bent 1,4-diphenoxide (∠Ti−O6A−C16 = 129.3(3)°) ligand has a longer titanium−oxygen distance ($d$(Ti−O6A) = 1.923(3) Å) because it is hydrogen bonded[60] with a 4-hydroxyphenoxide ($d$(Ti−O4A) = 2.207(3) Å) ligand that is also kinked (∠Ti−O4A−C10 = 125.9(3) Å). To hydrogen bond properly, the latter two ligands are tipped toward each other (∠O1−Ti−O4A = 81.5(2)°, ∠O1−Ti−O6A = 85.5(2)°, ∠O1A−Ti−O4A = 76.4(2)°, ∠O1A−Ti−O6A = 89.4(2)°).

In Figure 2, the $\mu$-O-1,4-hydroxyphenoxide groups that essentially fill void space have been removed for clarity, and

(58) (a) Svetich, G. W.; Voge, A. A. *J. Chem. Soc., Chem. Commun.* **1971**, 676−677. (b) Svetich, G. W.; Voge, A. A. *Acta Crystallogr.* **1972**, *B28*, 1760−1767.
(59) Watenpaugh, K.; Caughlan, C. N. *Inorg. Chem.* **1966**, *5*, 1782−1786.
(60) Vaarstra, B. A.; Huffman, J. C.; Gradeff, P. S.; Hubert-Pfalzgraf, L. G.; Daran, J.-C.; Parraud, S.; Yunlu, K.; Caulton, K. G. *Inorg. Chem.* **1990**, *29*, 3126−3131.

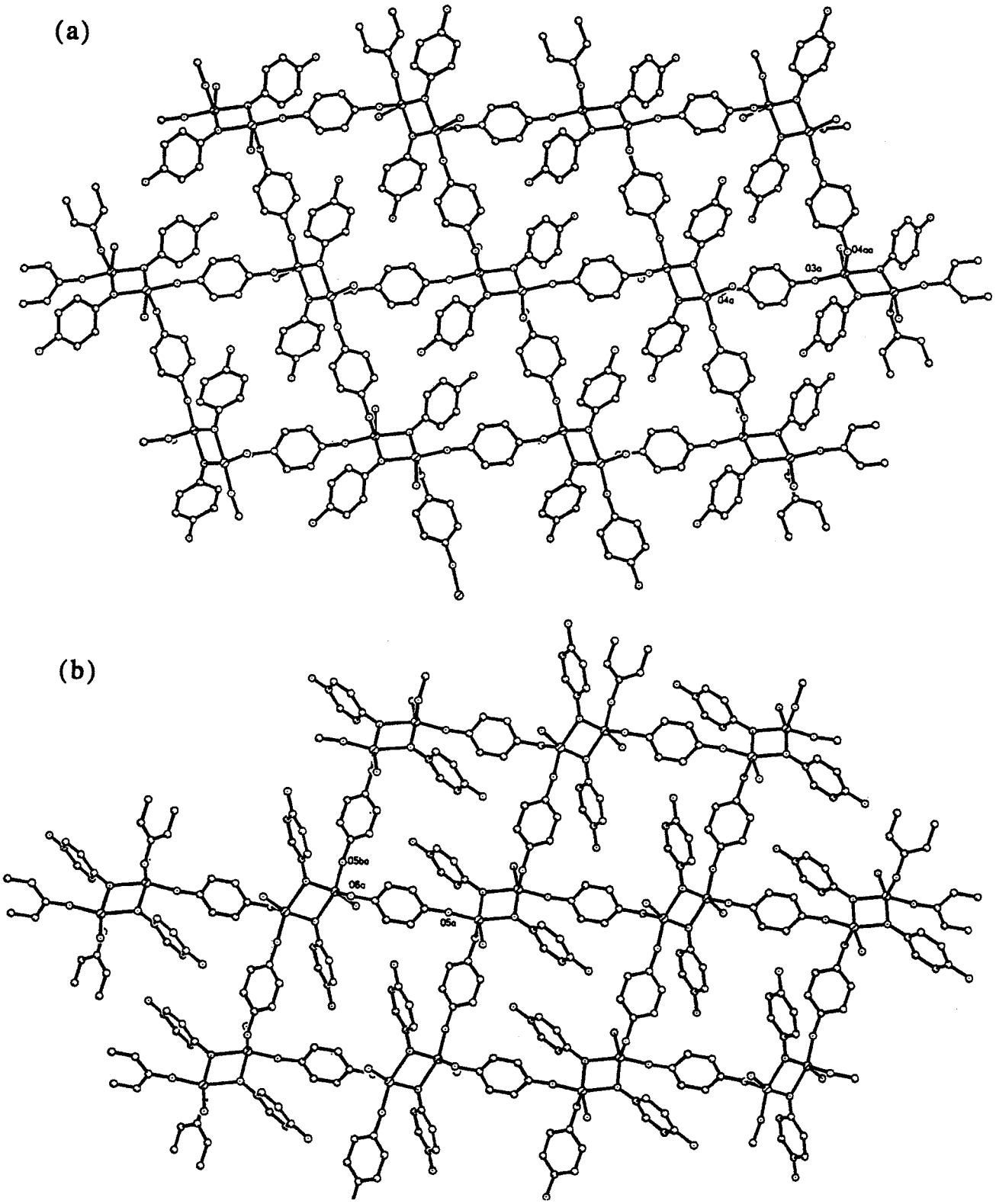


**Figure 3.** (a) 4-Hydroxyphenoxide (O3, O4) net of $[Ti_2(\mu_{1,4}-OC_6H_4O)_2(\mu_{1,4}-OC_6H_4OH)_2(\mu-OC_6H_4OH)_2]_\infty$ (**2**). (b) 1,4-Diphenoxide group (O5, O6) net of **2**.

the connectivity of the dititanium units is readily apparent. The $Ti_2(\mu-OC_6H_4OH)_2$ groups are linked via $\mu_{1,4}$-$OC_6H_4O$ and $\mu_{1,4}$-$OC_6H_4OH$ ligands that connect axial sites to equatorial sites ($Ti-O6A_{ax}-C_6H_4-O5_{eq}-Ti$; $Ti-(HO4A)_{ax}-C_6H_4-O3_{eq}-Ti$) on neighboring dititanium centers. The same connectivity can be used to describe a plane roughly perpendicular to the one depicted, thereby completing the 3-dimensional network. In another depiction, a net comprised of the 4-hydroxyphenoxide connectivity is shown with the inclusion of the $\mu$-$OC_6H_4OH$ groups (O3- - -O4 net, Figure 3a). When combined with the nearly equivalent net derived from the 1,4-diphenoxide group (O5- - -O6 net, Figure 3b), an alternative view of the 3-dimensional network is presented.

**3. $[Ti_2(\mu_{1,4}\text{-}OC_6H_4O)_2(\mu_{1,4}\text{:}\eta^2,\eta^1\text{-}OC_6H_4O)_2(OH_2)_2\cdot(H_2O)_2\cdot(HOC_6H_4OH)\cdot(Me\text{-}CN)]_\infty$ (4).** Figure 4 shows the bioctahedral dititanium building block of **4**, which possesses approximate—

**Table 2.** Selected Interatomic Distances (Å) and Angles (deg) in $[Ti_2(\mu_{1,4}\text{-}OC_6H_4O)_2(\mu_{1,4}\text{-}OC_6H_4OH)_2(\mu\text{-}OC_6H_4OH)_2]_\infty$ (**2**)

| | | | | | |
|---|---|---|---|---|---|
| Ti···TiA | 3.276 (2) | Ti−O5 | 1.794 (4) | O4−C10 | 1.386 (6) |
| Ti−O1 | 2.047 (3) | Ti−O6A | 1.923 (3) | O5−C13 | 1.352 (6) |
| Ti−O1A | 2.042 (3) | O1−C1 | 1.371 (6) | O6−C16 | 1.376 (6) |
| Ti−O3 | 1.782 (3) | O2−C4 | 1.373 (7) | $(C-C)_{ave}$ | 1.382 (8) |
| Ti−O4A | 2.207 (3) | O3−C7 | 1.361 (6) | | |
| O1−Ti−O1A | 73.5 (2) | O1A-Ti−O6A | 89.4 (2) | Ti−O1−C1 | 126.2 (3) |
| O1−Ti−O3 | 166.2 (2) | O3−Ti−O4A | 92.2 (2) | Ti−O1A−C1 | 126.8 (3) |
| O1−Ti−O4A | 81.5 (2) | O3−Ti−O5 | 99.8 (2) | Ti−O3−C7 | 173.0 (3) |
| O1−Ti−O5 | 92.5 (2) | O3−Ti−O6A | 98.0 (2) | Ti−O4A−C10 | 125.9 (3) |
| O1−Ti−O6A | 85.5 (2) | O4A-Ti−O5 | 89.3 (2) | Ti−O5−C13 | 164.1 (3) |
| O1A−Ti−O3 | 93.1 (2) | O4A-Ti−O6A | 163.0 (2) | Ti−O6A−C16 | 129.3 (3) |
| O1A−Ti−O4A | 76.4 (2) | O5−Ti−O6A | 102.3 (2) | $(O-C-C)_{ave}$ | 120.1 (14) |
| O1A−Ti−O5 | 161.1 (2) | Ti−O1−Ti | 106.5 (2) | $(C-C-C)_{ave}$ | 120.0 (8) |

**Table 3.** Selected Interatomic Distances (Å) and Angles (deg) in $[Ti_2(\mu_{1,4}\text{-}OC_6H_4O)_2(\mu_{1,4}:\eta_2,\eta_1\text{-}OC_6H_4O)_2(OH_2)_2\cdot(H_2O)_2\cdot(HOC_6H_4OH)\cdot(MeCN)]_\infty$ (**4**)

| | | | | | |
|---|---|---|---|---|---|
| Ti(1)−O(1) | 1.836 (8) | Ti(2)−O(1B) | 2.072 (8) | O(1)···O(2S) | 2.83 (2) |
| Ti(1)−O(1B) | 2.014 (7) | Ti(2)−O(2B) | 2.020 (8) | O(1W)···O(1S) | 2.83 (2) |
| Ti(1)−O(2) | 1.808 (9) | Ti(2)−O(5) | 2.186 (10) | O(1W)···O(2S) | 2.99 (2) |
| Ti(1)−O(2B) | 2.076 (8) | Ti(2)−O(6) | 1.795 (9) | O(1W)···O(3) | 2.73 (2) |
| Ti(1)−O(3) | 2.187 (9) | Ti(2)−O(7) | 1.814 (7) | O(1S)···N(1) | 2.76 (2) |
| Ti(1)−O(4) | 1.785 (9) | Ti(2)−O(8) | 1.855 (9) | O(2)···O(5) | 3.03 (2) |
| $(C-O)_{ave}$ | 1.37 (2) | $(C-C)_{ave}$ | 1.39 (2) | O(3)···O(8) | 2.74 (2) |
| Ti(1)···Ti(2) | 3.297 (3) | | | O(5)···O(2W) | 2.65 (2) |
| O1−Ti1−O1B | 162.1 (4) | O1B−Ti2−O2B | 72.4 (3) | Ti1−O1B−Ti2 | 107.6 (4) |
| O1−Ti1−O2 | 94.6 (4) | O1B−Ti2−O5 | 79.8 (3) | Ti1−O2B−Ti2 | 107.2 (4) |
| O1−Ti1−O2B | 91.3 (3) | O1B−Ti2−O6 | 165.0 (4) | Ti1−O1−C13 | 140.4 (8) |
| O1−Ti1−O3 | 86.3 (4) | O1B−Ti2−O7 | 93.0 (3) | Ti1−O1B−C1 | 126.6 (7) |
| O1−Ti1−O4 | 99.2 (4) | O1B−Ti2−O8 | 88.6 (4) | Ti1−O2−C19 | 146.8 (9) |
| O1B−Ti1−O2 | 92.8 (4) | O2B−Ti2−O5 | 78.0 (3) | Ti1−O2B−C10A | 124.5 (7) |
| O1B−Ti1−O2B | 72.4 (3) | O2B−Ti2−O6 | 94.4 (4) | Ti1−O4−C4A | 152.3 (7) |
| O1B−Ti1−O3 | 83.7(3) | O2B−Ti2−O7 | 160.6 (4) | Ti2−O1B−C1 | 125.7 (7) |
| O1B−Ti1−O4 | 95.4 (4) | O2B−Ti2−O8 | 90.8 (3) | Ti2−O2B−C10A | 127.7 (7) |
| O2−Ti1−O2B | 90.0 (4) | O5−Ti2−O6 | 90.8 (4) | Ti2−O6−C7 | 144.0 (7) |
| O2−Ti1−O3 | 169.9 (4) | O5−Ti2−O7 | 87.0 (4) | Ti2−O7−C16A | 147.0 (9) |
| O2−Ti1−O4 | 100.3 (4) | O5−Ti2−O8 | 165.8 (3) | Ti2−O8−C22 | 134.2 (8) |
| O2B−Ti1−O3 | 79.9 (3) | O6−Ti2−O7 | 98.1 (4) | $(O-C-C)_{ave}$ | 120.1 (10) |
| O2B−Ti1−O4 | 164.6 (4) | O6−Ti2−O8 | 98.8 (4) | $(C-C-C)_{ave}$ | 120.0 (11) |
| O3−Ti1−O4 | 89.4 (4) | O7−Ti2−O8 | 102.0 (4) | | |

but not crystallographic—inversion symmetry. The titanium−titanium distance of 3.297 (3) Å is near that in **2** (3.276 (2) Å), and the coordination is also similar, except that each Ti has a bound water ($d(Ti-OH_2)_{ave}$ = 2.187(1) Å), and all other linkages are either terminal ($d(Ti-O_t)_{ave}$ = 1.82(2) Å) or bridging ($d(Ti-O_b)_{ave}$ = 2.06(3) Å) titanium phenoxides. The angles that describe the equatorial plane are within 1.8° of the related angles in **2** and are listed in Table 3. Axial waters are within hydrogen bonding distance to adjacent 1,4-diphenoxide ligands ($d$(O3···O8) = 2.74 (1) Å, $d$(O2···O5) = 3.03 Å) in **4**, replacing the axial 1,4-diphenoxide/4-hydroxyphenoxide hydrogen-bonded framework of **2**. The axial phenoxides (O2, O8) are essentially normal ($\angle O_b-Ti-O_{ax}(Ph)$ = 90.6(18)°) to the $Ti_2O_2$ core, while the waters (O3, O5) lean toward their phenoxide partners ($\angle O_b-Ti-O_{ax}(W)$ = 80.4(24)°).

While the channels of the solid state compound are relatively large compared with **2**, a complex hydrogen-bonding network is present that links the solvate molecules with the covalent net (Figure 5). Each of the coordinated waters is hydrogen bonded to a water of crystallization ($d$(O5···O2W) = 2.65(2) Å, $d$(O3···O1W) = 2.73(2) Å, and lattice water O1W is also hydrogen bonded to two types of hydroquinone of crystallization ($d$(O1W···O1S) = 2.83(2) Å, $d$(O1W···O2S)) = 2.99(2) Å). One-half of each hydroquinone is part of the asymmetric unit, hence there is only one total $HOC_6H_4OH$ unit incorporated within the lattice. One hydroquinone also hydrogen bonds to the acetonitrile ($d$(O1S···N1) = 2.76(2) Å), while the other also hydrogen bonds to a 1,4-diphenoxide ligand ($d$(O1···O2S) = 2.83(2) Å), thus both hydroquinones are involved in four hydrogen bonds—two for each oxygen. The second water of solvation, O2W, does not have additional conventional hydrogen bonding interactions, but appears to hydrogen bond to the $\pi$-system of a hydroquinone.

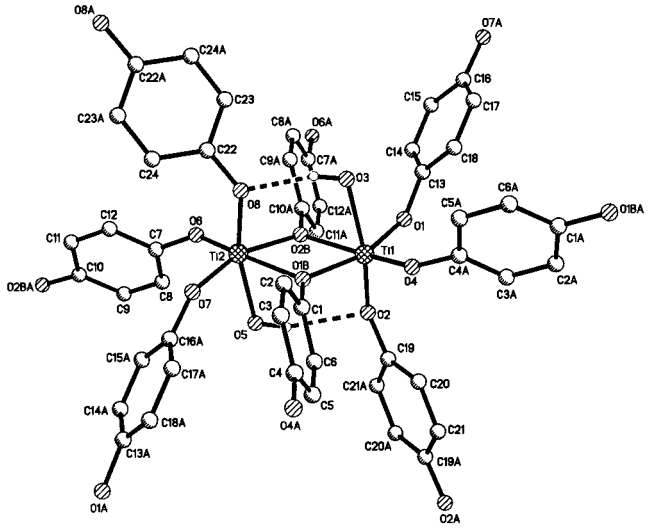


**Figure 4.** Bioctahedral dititanium building block of $[Ti_2(\mu_{1,4}\text{-}OC_6H_4O)_2(\mu_{1,4}:\eta_2,\eta_1\text{-}OC_6H_4O)_2(OH_2)_2\cdot(H_2O)_2\cdot(HOC_6H_4OH)\cdot(MeCN)]_\infty$ (**4**).

The 1,4-diphenoxides in the dititanium building block, the terminal and the two $\mu_{1,4}$:$\eta^2$,$\eta^1$-$OC_6H_4O$ ligands, connect with

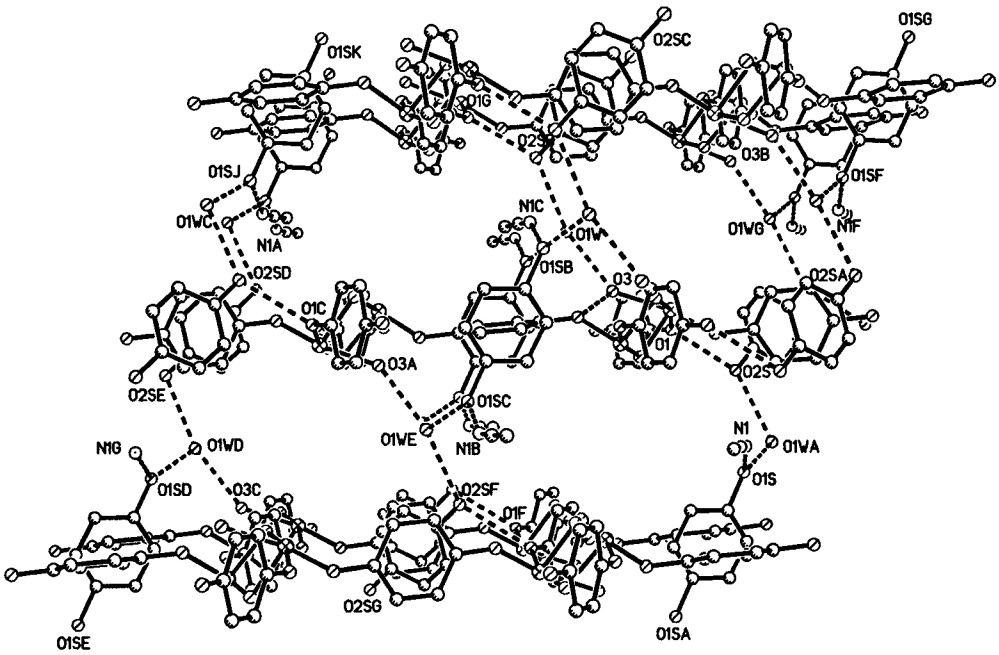


**Figure 5.** Hydrogen-bonding network of $[Ti_2(\mu_{1,4}\text{-}OC_6H_4O)_2(\mu_{1,4}\text{:}\eta_2,\eta_1\text{-}OC_6H_4O)_2(OH_2)_2\cdot(H_2O)_2\cdot(HOC_6H_4OH)\cdot(MeCN)]_\infty$ (**4**).

**Table 4.** Selected Interatomic Distances (Å) and Angles (deg) in $[Ti_2(\mu_{1,7}\text{-}OC_{10}H_6O)_2(\mu_{1,7}\text{:}\eta_2,\eta_1\text{-}OC_{10}H_6OH)_2(O^iPr)_2]_\infty$ (**5**)

| | | | | | |
|---|---|---|---|---|---|
| Ti···TiA | 3.392 (2) | Ti−O4 | 1.835 (4) | O4−C17 | 1.357 (5) |
| Ti−O1 | 2.258 (3) | Ti−O5 | 1.751 (3) | O5−C21 | 1.441 (6) |
| Ti−O2A | 2.070 (3) | O1−C1 | 1.383 (6) | $(C-C)_{Np\ ave}$ | 1.40 (3) |
| Ti−O2B | 2.082 (3) | O2−C5 | 1.374 (5) | C21−C22 | 1.499 (7) |
| Ti−O3 | 1.892 (3) | O3−C11 | 1.370 (6) | C21−C23 | 1.521 (8) |
| | | | | O1···O3 | 2.75 (1) |
| O1−Ti−O2A | 76.5 (2) | O2B−Ti−O3 | 87.0 (2) | Ti−O2B−C5 | 125.5 (3) |
| O1−Ti−O2B | 78.6 (2) | O2B−Ti−O4 | 90.9 (2) | Ti−O3−C11 | 141.0 (3) |
| O1−Ti−O3 | 162.2 (2) | O2B−Ti−O5 | 162.7 (2) | Ti−O4−C17 | 140.0 (3) |
| O1−Ti−O4 | 89.1 (2) | O3−Ti−O4 | 97.9 (2) | Ti−O5−C21 | 173.2 (3) |
| O1−Ti−O5 | 92.6 (2) | O3−Ti−O5 | 101.8 (2) | $(O-C-C)_{Np\ ave}$ | 119.8 (14) |
| O2A−Ti−O2B | 70.4 (2) | O4−Ti−O5 | 102.5 (2) | $(C-C-C)_{Np\ ave}$ | 120.1 (21) |
| O2A−Ti−O3 | 89.8 (2) | Ti−O2−Ti | 109.6 (2) | O5−C21−C22 | 109.7 (4) |
| O2A−Ti−O4 | 159.5 (2) | Ti−O1−C1 | 133.0 (2) | O5−C21−C23 | 108.8 (4) |
| O2A−Ti−O5 | 94.4 (2) | Ti−O2A−C5 | 124.8 (3) | C22−C21−C23 | 112.2 (4) |

eight neighboring dititanium cores. Utilization of the latter connectivity differentiates **4** from **2**, and changes the structural motif into a 3-dimensional parallelepiped, with one side halved by a diagonal connection. The net shown in Figure 6a is the simplest to view, arising from alternating axial (relative to the equatorial $(RO)_2Ti(\mu\text{-}OR)_2Ti(OR)_2$ core) connections involving terminal, symmetrical -O(2)$C_6H_4$O(2)- and -O(8)$C_6H_4$O(8)- bridges in one dimension, and an equatorial -O(1)$C_6H_4$O(7)- connectivity in the other. The parallelogram motif in Figure 6b is composed of linkages utilizing the $\mu_{1,4}\text{:}\eta^2,\eta^1\text{-}OC_6H_4O$ ligands; both dimensions are described by a head-to-head, tail-to-tail alternation of $\mu$-O(1B)$C_6H_4$O(4)- and $\mu$-O(2B)$C_6H_4$O(6)- bridges confined to the equatorial plane. The equatorial -O(1)$C_6H_4$O-(7)- bridge connects pseudo orthogonal $Ti_2O_2$ cores across the short diagonal. A third net, not shown, combines the structural elements of the previous two to compose the third parallelogram of the 3-dimensional material.

**4. $[Ti_2(\mu_{1,7}\text{-}OC_{10}H_6O)_2(\mu_{1,7}\text{:}\eta^2,\eta^1\text{-}OC_{10}H_6OH)_2(O^iPr)_2]_\infty$ (5).** Due to a moderate amount of quality data, structure solution was accomplished via isotropic refinement of all atoms except Ti, which was refined anisotropically. Given the rigid nature of the organic spacer and lattice, this was not considered a serious detriment to the study, and all geometric facets of the structure solution appear reasonable (Table 4).

Figure 7 illustrates yet another dititanium building block—this one pertaining to **5**—which manifests inversion symmetry about the 3.392(2) Å intertitanium spacing. The coordination environment of **5** is also similar to **2**, with the majority of its core angles within 4°, and related bridging, equatorial terminal, axial terminal and phenolic Ti−O distances of $2.076(9)_{ave}$, 1.835(4), 1.892(3), and 2.210 Å. The 2.75(1) Å distance between the axial aryloxide and phenolic oxygens (O1−O3B) is consistent with a hydrogen bond,[60] and the unique titanium−isopropoxide bond length of 1.751(3) Å is normal.

The dititanium unit contains eight connectors to its nearest neighbors: two terminal $\mu_{1,7}\text{-}OC_{10}H_6O$ diaryloxides that are attached at both ends, and two $\mu_{1,7}\text{:}\eta^2,\eta^1\text{-}OC_{10}H_6OH$ groups linked at the aryloxide position in the bridge and at the phenolic functionality in a terminal site. A view down the *a* axis (Figure 8) illustrates the 3-dimensionality of the lattice, and reveals relatively small channels that are partially filled by isopropoxide units. This network is best described by viewing the connectivity in two segments. The spiral network depicted in Figure 9a is derived from efficient packing of the 2,7-dinaphthaloxide ligand, which connects axial O3 sites to equatorial O4 sites of adjacent dititanium units. Because the dititanium block contains a center of symmetry, the two dimensions of the net are composed of

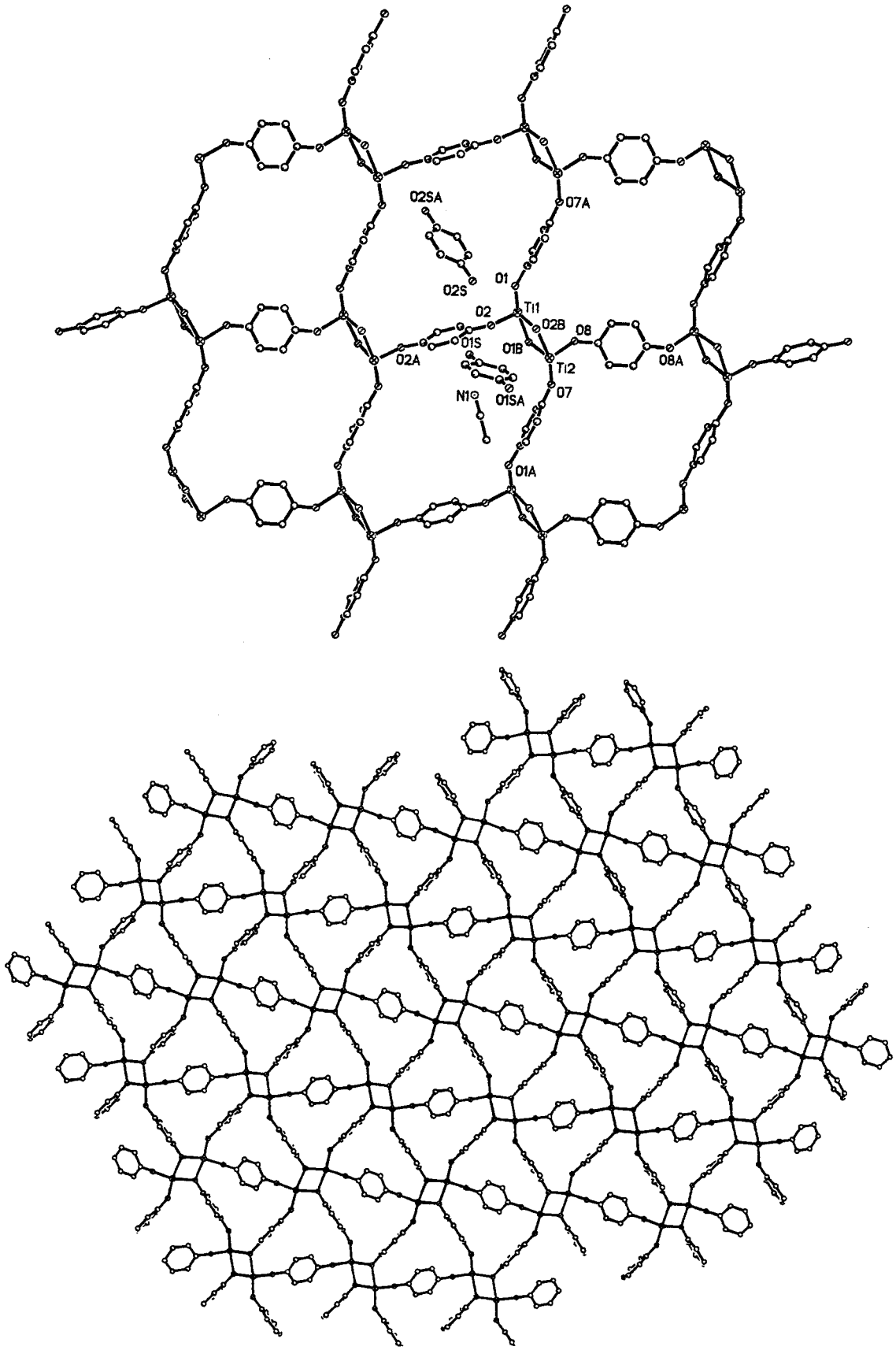


**Figure 6.** (a) One parallelogram net of $[Ti_2(\mu_{1,4}\text{-}OC_6H_4O)_2(\mu_{1,4}{:}\eta_2,\eta_1\text{-}OC_6H_4\text{-}O)_2(OH_2)_2{\cdot}(H_2O)_2{\cdot}(HOC_6H_4OH){\cdot}(MeCN)]_\infty$ (**4**). Aryl portions of the bridges and aryloxides inconsequential to the net have been removed; the two independent hydroquinones (crystallographically, two unique halves) and acetonitrile have been included only once for clarity. (b) Triangular connectivity of **4**. When combined with a second parallelogram net similar to that in (a), a hexagonal motif is apparent.

identical $[O3\cdots O4Ti\cdots TiO4'\cdots O3']_n$, S-curved connectivites. The isopropoxides extend above and below this net into the open sections of the lattice. The remaining parallelogram network, shown in Figure 9b, contains two identical strands of

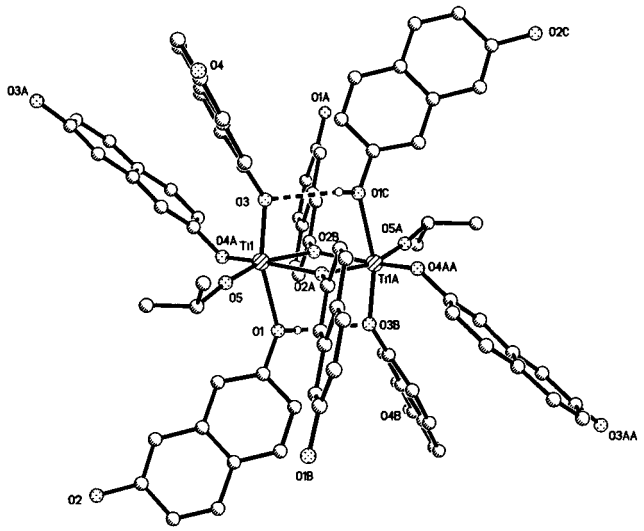


**Figure 7.** Bioctahedral dititanium building block of $[Ti_2(\mu_{1,7}\text{-}OC_{10}H_6\text{-}O)_2(\mu_{1,7}\text{:}\eta_2,\eta_1\text{-}OC_{10}H_6OH)_2(O^iPr)_2]_\infty$ (**5**).

the $\mu_{1,7}$:$\eta^2$,$\eta^1$-$OC_{10}H_6OH$ connector linked in a head-to-head (i.e., ($\mu$-O2)Ti···Ti($\mu$-O2′)), tail-to-tail (i.e., $(O1_{ax})$Ti···Ti$(O1'_{ax})$ fashion.

## Discussion

**Crystallization and Annealing.** The desolvation of molecular species or charged ions, and their aggregation into a critical size where lattice energy and related solid-state properties become relevant in describing the material, is a standard view of the crystallization event. Corrections in the growing lattice occur via the dynamic equilibrium between the solid and its solvated components. Provided donor−acceptor bonds are the linkages in metal-organic networks, crystallization can be viewed in similar light, but in the 3-dimensional CMON compounds above, this growth scenario is incommensurate with the nature of the titanium-aryloxide covalent bonds. Growth and degradation of the networks derive from an alcoholysis reaction that swaps −OH for −OTi bonds via proton-transfer pathways in $X_nTi(OR)(HOR')$ intermediates. In a sense, the synthesis of CMON materials is related to conventional, "from the elements" solid-state syntheses. In either, covalent bonds not intrinsic to the product are made and broken during the course of synthesis.

While these subtleties of materials synthesis may seem trivial, in practice the inability to recrystallize a material, as in molecular or salt crystallizations, has proven to be a serious detriment to obtaining single crystal sizes amenable to X-ray diffraction analysis. Since a chemical reaction, alcoholysis, is required to degrade a CMON material, efforts at regrowing or annealing a

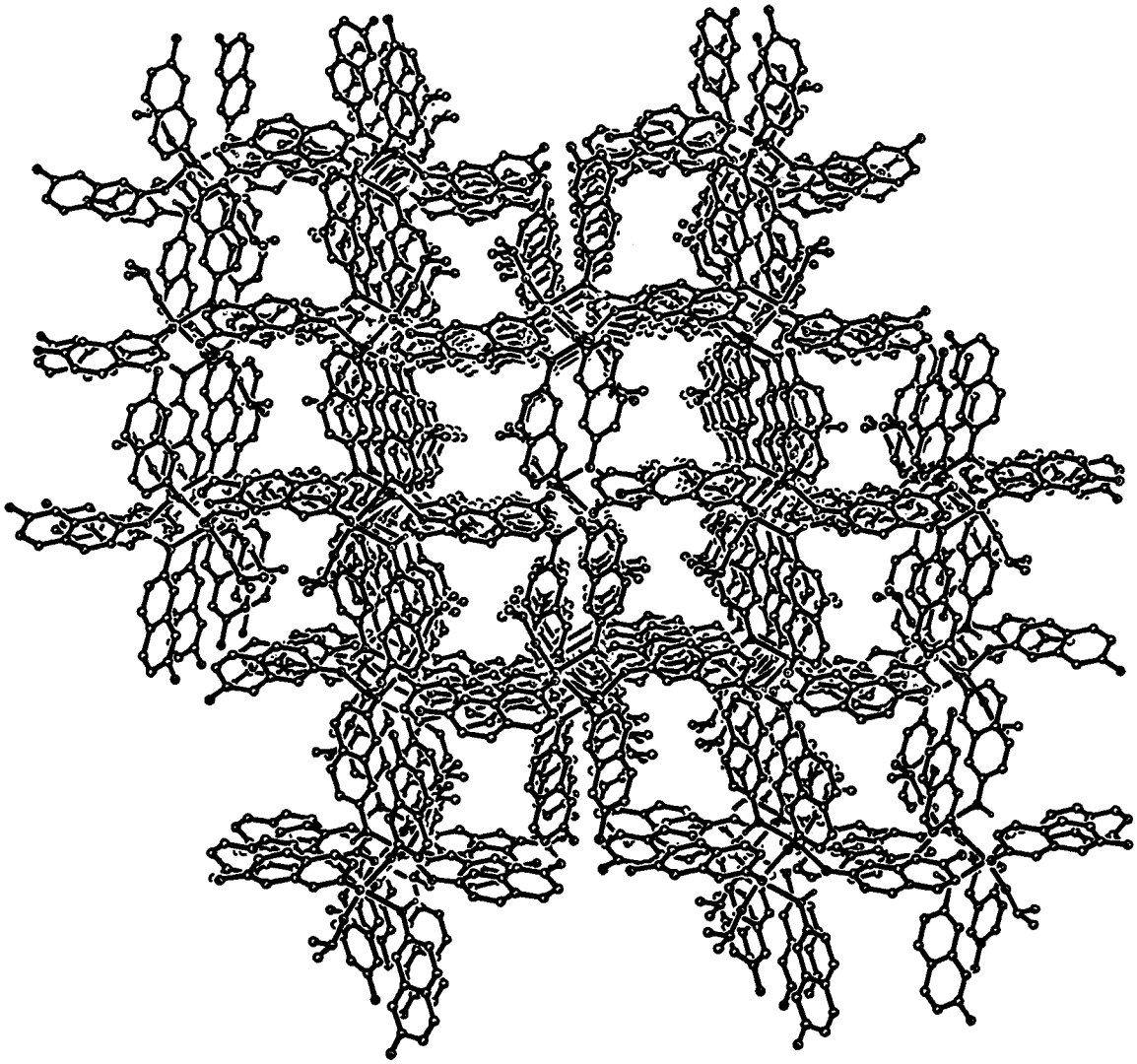

**Figure 8.** View down the *a* axis of $[Ti_2(\mu_{1,7}\text{-}OC_{10}H_6\text{-}O)_2(\mu_{1,7}\text{:}\eta_2,\eta_1\text{-}OC_{10}H_6OH)_2(O^iPr)_2]_\infty$ (**5**), illustrating the dense network and corresponding small channels.

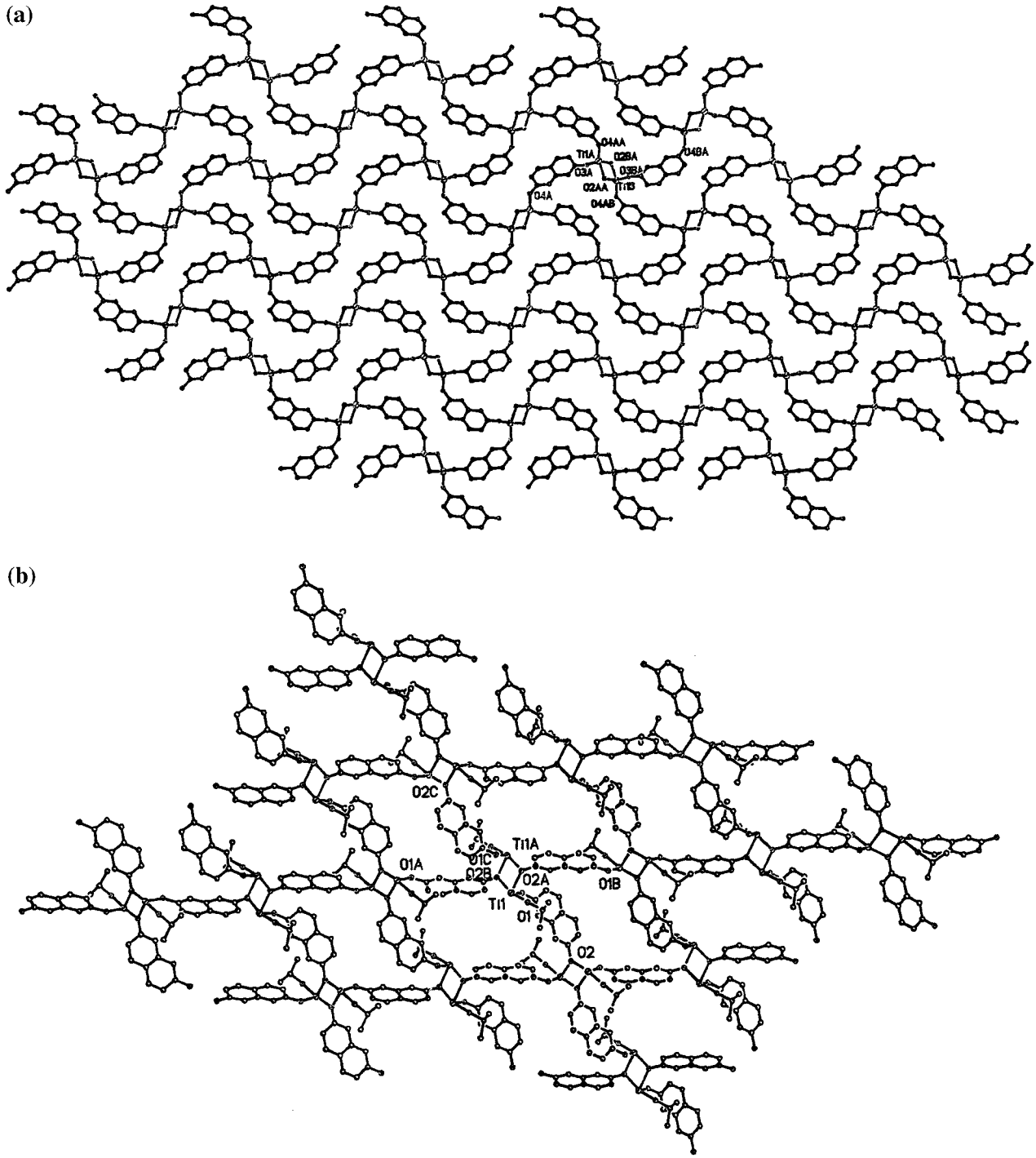


**Figure 9.** (a) Spiral O3−O4 network of $[Ti_2(\mu_{1,7}\text{-}OC_{10}H_6\text{-}O)_2(\mu_{1,7}{:}\eta_2,\eta_1\text{-}OC_{10}H_6OH)_2(O^iPr)_2]_\infty$ (**5**); the isopropoxides and the bridging aryl and axial O1 connectors have been removed for clarity. (b) Head-to-head (O2), tail-to-tail (O1) network of **5**; the axial O3 and equatorial O4 connections have been removed for clarity.

species is tantamount to resynthesizing the compound. Nonetheless, once a greater understanding of the growth process can be obtained, it may be possible to use the vicissitudes of alcoholyses and complementary reactions to improve annealing methodology, principally by facilitating alkoxide/alcohol exchange.

**Structural Comparisons. 1. Primary Structure.** The dititanium, bioctahedral building block is common to the three compounds (**2**, **4**, and **5**) characterized by X-ray crystallography, and its structural features provide the primary structure critical to formation of the 3-dimensional networks. In each structure, axial aryloxide and aryl-hydroxide or water ligands buttress the bridging aryloxides via hydrogen bonding,[60] thereby solidifying

∠Ti-$O_b$-Ti = 107.7 (13)
∠$O_b$-Ti-$O_{b'}$ = 72.2 (13)
∠$O_b$-Ti-$O_{eq}$ = 93.1 (16)
∠$O_b$-Ti-$O'_{eq}$ = 162.7 (24)
∠$O_{eq}$-Ti-$O'_{eq}$ = 99.9 (19)
∠$O_b$-Ti-$O_{ax}$ = 89.2 (23)
∠$O_b$-Ti-$O_{ax}$(H) = 79.3 (25)
∠$O_{ax}$-Ti-$O_{eq}$ = 99.5 (27)
∠$O_{ax}$(H)-Ti-$O_{eq}$ = 89.6 (22)
∠$O_{ax}$-Ti-$O_{ax}$(H) = 165.2 (35)

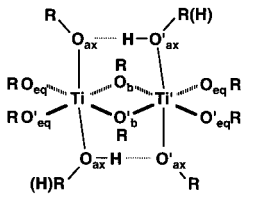


d(Ti-$O_b$) = 2.053 (26)
d(Ti-$O_{eq}$) = 1.806 (23)
d(Ti-$O_{ax}$) = 1.870 (50)
d(Ti-$O_{ax}$H) = 2.210 (34)

**Figure 10.** Common core of the bioctahedral dititanium building block.

the junction of the two octahedra. Figure 10 illustrates the dititanium core, including bond angles and bond distances obtained by averaging common geometric quantities of the three

structures. Given the regular nature of octahedral coordination around titanium, it was not surprising to find similar conformations, but the degree to which **2**, **4**, and **5** possess related dititanium geometric features was not anticipated, especially considering the disparate natures of the networks. The bond distance with greatest deviation—that describing the Ti−$O_{ax}$ bond—only has a $\sigma$ of 0.05 Å, while the largest $\sigma$ among the bond angles is a mere 3.5°. In addition, there exists a one-to-one correspondence of $[(PhO)_3(PhOH)Ti]_2(\mu\text{-}OPh)_2$[58] to the average core in Figure 10. Its titanium−oxygen distances are within 0.04 Å, and all of the critical core angles are within 3 degrees. The dititanium unit must be considered a natural building block for a 3-dimensional network, and none of its general geometric features are considered a consequence of the extended nature of the compound.

**2. Secondary Structure.** The secondary structures of the 3-dimensional networks derive from the nature of the connecting aryloxide/hydroxide functionality, and the disposition of the linking agents about the dititanium unit. Interpenetrating networks are not observed,[4,5] perhaps as a consequence of the limited dynamics of the alcoholysis process. Instead, high densities are achieved due to efficient packing (**2**, **5**) or through a combination of packing and the inclusion of small molecules (**4**).

To simplify the secondary connectivity so that it can be easily understood, it is pertinent to view each dititanium bioctahedron as a single point. In $[Ti_2(\mu_{1,4}\text{-}OC_6H_4O)_2(\mu_{1,4}\text{-}OC_6H_4OH)_2(\mu\text{-}OC_6H_4OH)_2]_\infty$ (**2**), the approximately symmetric arrangement of the eight spanning 1,4-diphenoxide and 4-hydroxyphenoxide ligands yields a relatively regular structure that possesses a pseudo body-centered motif of dititanium centers. Figure 2 exhibits the regularity in the secondary structure, revealing networks composed of body diagonals, while Figure 3 illustrates diamondoid networks derived from individual connectors.

A dramatic change in secondary structure is evident in $[Ti_2(\mu_{1,4}\text{-}OC_6H_4O)_2(\mu_{1,4}\text{:}\eta^2,\eta^1\text{-}OC_6H_4O)_2(OH_2)_2\cdot(H_2O)_2\cdot(HOC_6H_4OH)\cdot(MeCN)]_\infty$ (**4**). Each dititanium unit has six connections within a single plane, as illustrated in Figure 6b, and two additional linkages occurring above and below this plane (Figure 6a), hence this structure can be considered as pseudohexagonal.

A return to a body-centered motif is realized in the structure of $[Ti_2(\mu_{1,7}\text{-}OC_{10}H_6O)_2(\mu_{1,7}\text{:}\eta^2,\eta^1\text{-}OC_{10}H_6OH)_2(O^iPr)_2]_\infty$ (**5**), but the nature of the secondary connections is difficult to recognize given the curved connectivity intrinsic to the 2,7-dialkoxynaphthalene ligand. The view of the parallelogram network in Figure 9b minimizes this curvature and the two body diagonals are readily discerned, but the body diagonals in Figure 9a are somewhat obfuscated by this view in which the naphthalene backbones of the connectors are virtually planar.

## Conclusions

Alcoholysis has proven to be a useful method of producing covalent, metal-organic network (CMON) solids based on dititanium cores linked by aryloxide ligands, although the nature of the crystallization renders crystal growth difficult. When the solvent is a poor ligand, dense 3-dimensional networks are generated, in part because titanium achieves octahedral coordination by dimerizing via $\mu$-OAr coordination. Secondary structural motifs of CMON compounds can be rationalized on close-packing arrays related to simple solid state species. Characterization of the CMON materials is dependent on the ability to grow crystals large enough to assay by single-crystal XRD. The use of high-energy X-ray sources partly offsets such difficulities, but the percentage of characterizable materials is still well under 10%. The effect of donor capacity and aryloxide size on the dimensionality of CMON materials is under investigation as the scope and chemistry of this new class of compounds continues to be investigated.

## Experimental Section

**General Considerations.** Ethereal solvents were distilled from purple sodium benzophenone ketyl and then vacuum transferred from the same immediately prior to use. Pyridine was dried by refluxing over sodium and stored over 4 Å molecular seives. Acetonitrile was dried by stirring over $P_2O_5$ and stored over 4 Å molecular seives. Hydroquinone (Aldrich, 99+%) was dried by dissolving it in dry THF and then removing the volatiles; this procedure was repeated three times sequentially. $Ti(O^iPr)_4$ was used as received (Aldrich, 97%) and stored in the drybox. DCl (20 wt % in $D_2O$, Aldrich) and $D_2O$ were used as received; solutions for $^1$H NMR were ca. 3 wt % DCl (~1 M).

$^1$H NMR spectra were obtained on Varian XL-200 spectrometer. Spectra were the product of 4 transients with a 60 s delay between acquisitions to ensure accurate integrations. Infrared spectra were taken on a Nicolet Impact 410 spectrometer interfaced to a Gateway 2000 computer. Powder diffraction was performed on a Scintag XRD system interfaced to a Digital MicroVax computer or PC with Windows NT. Standard powder patterns were recorded as continuous scans with a chopper increment of 0.03° 2$\theta$ and a scan rate of 2° per minute. Patterns for indexing and refinement of unit cell parameters were recorded at 0.03° steps in 2$\theta$, with diffraction recorded for at least 30 s at each step. Patterns were indexed using TREOR or VISSER and unit cell constants were refined using LATCON, all part of the Proszki suite of programs.

**Procedures. 1. Preparation of $[Ti(OC_6H_4O)_a(OC_6H_4OH)_{3.33-1.83a}(O^iPr)_{0.66-0.17a}(THF)_{\sim 0.2}]_n$ (1).** Hydroquinone (5.00 g, 45.4 mmol) was placed in a 100 mL flask on a swivel frit. $Ti(O^iPr)_4$ (5.00 g, 17.6 mmol) was placed in a 100 mL flask connected to a 180° needle valve. THF (~30 mL) was vacuum transferred into each flask to form colorless solutions. The $Ti(O^iPr)_4$ was taken into a 60 mL syringe and added to the hydroquinone solution at 22 °C with stirring. A large red-orange solid clump formed and was subsequently broken up to a powder by stirring for 3 h at 22 °C. The suspension was filtered and the volatiles removed. Red-orange powder was left under active vacuum for 96 h. $^1$H NMR of the solid dissolved in $D_2O$/DCl yielded the empirical formula $Ti(OC_6H_4O)_a(OC_6H_4OH)_{3.33-1.83a}(O^iPr)_{0.66-0.17a}(THF)_{\sim 0.2}$ ($0.90 \le a \le 1.82$) based on ratios of hydroquinone CH, $^i$PrOH, and THF resonances. The composition of **1** was assessed each time it was prepared, and its compositional range is given on the basis of the quenches.

**2. Preparation of $[Ti_2(\mu_{1,4}\text{-}OC_6H_4O)_2(\mu_{1,4}\text{-}OC_6H_4OH)_2(\mu\text{-}OC_6H_4OH)_2]_\infty$ (2).** Hydroquinone (3.00 g, 27.2 mmol), 500 mg of **1**, and 20 mL of ether were combined in a glass bomb and heated to 100 °C for 48 h. The resulting red microcrystals were collected on a glass frit on the benchtop, washed with ether, and placed under vacuum for 15 min. Crystals are red parallelograms up to 15 × 15 × 50 $\mu$m in size. $^1$H NMR indicated the presence of a trace of ether (1:0.025 ratio of quinone to ether). A powder pattern of the bulk materials matched that generated from the single-crystal XRD study (see Supporting Information). IR (Nujol, cm$^{-1}$): 3464 (w), 3425 (w), 1212 (s), 1201 (s), 1091 (w), 1017 (w), 908 (s), 830 (s), 776 (m), 659 (w), 644 (w), 608 (m), 554 (w), 521 (w), 493 (m), 482 (w), 461 (m), 418 (w). Anal. Calcd (found): C, 57.78 (55.42); H, 3.77 (3.10).

**3. Preparation of $[Ti(OC_6H_4O)_{2-a}(OC_6H_4OH)_{2a}(THF)_{0.20(2+a)}]_n$ (3).** Hydroquinone (800 mg, 7.27 mmol), 100 mg of **1**, and ca. 3 mL of THF were combined in a glass bomb and heated to 100 °C for 48 h. Red microcrystals were isolated by filtration and washing with THF on the benchtop. The solid was placed under active vacuum for 15 min. When the solid was dissolved in $D_2O$/DCl, it yielded a $^1$H NMR that implied the formula $Ti(OC_6H_4O)_{2-a}(OC_6H_4OH)_{2a}(THF)_{0.20(2+a)}$. Crystals were rectangular and typically 5 × 15 $\mu$m.

**4. Preparation of $[Ti_2(\mu_{1,4}\text{-}OC_6H_4O)_2(\mu_{1,4}\text{:}\eta^2,\eta^1\text{-}OC_6H_4O)_2(OH_2)_2\cdot(H_2O)_2\cdot(HOC_6H_4OH)\cdot(MeCN)]_\infty$ (4).** Hydroquinone (3.00 g, 27.2 mmol, Aldrich 99%, *undried*), 500 mg of **1**, and 20 mL of acetonitrile were combined in a glass bomb and heated to 100 °C for 48 h. The resulting red microcrystals were collected on a glass frit on the benchtop,

washed with acetonitrile, and placed under vacuum for 15 min. $^1$H NMR integration of the DCl/$D_2O$ quench yielded a quinone-to-acetonitrile ratio of 5:2.0, a number not consistent with the single-crystal structure. Crystals were observed under a microscope to be red, hexagonal plates of varying size, up to 100 $\mu$m across, with good quality crystals up to 30 $\mu$m across. A powder pattern of the bulk materials matched that generated from the single-crystal XRD study (see Supporting Information). IR (Nujol, $cm^{-1}$): 3351 (m, broad), 2309 (w), 2283 (w), 1248 (m), 1240 (m), 1205 (vs), 1048 (w), 892 (m), 882 (m), 853 (s), 827 (s), 758 (w), 645 (w), 610 (w), 558 (m), 493 (s), 468 (m), 450 (s), 440 (s), 426 (m). Anal. Calcd for $Ti_2(OC_6H_4O)_4(HOC_6H_4OH)(CH_3CN)_2(H_2O)_4$ (found): C, 51.60 (56.92); H, 4.46 (3.41); N, 3.54 (3.39).

**5. Preparation of $[Ti_2(\mu_{1,7}\text{-}OC_{10}H_6O)_2(\mu_{1,7}\text{:}\eta^2,\eta^1\text{-}OC_{10}H_6OH)_2(O^iPr)_2]_\infty$ (5).** Excess 2,7-dihydroxynaphthalene (0.35 g, 2.2 mmol) in 2 mL of ether was treated with $Ti(O^iPr)_4$ (0.15 g, 0.53 mmol) in a glass tube, and an orange solid immediately precipitated. The tube was sealed under vacuum and heated for 7 d at 100 °C. Orange crystals were observed. After being heated for a total of 30 days, the product was collected by filtration in a glovebox and washed with THF several times to remove excess 2,7-dihydroxynaphthalene. The crystals were dried under vacuum for 30 m. Inspection of a sample immersed in Paratone oil by light microscopy revealed the crystals to be very thin orange plates of various shapes. A powder pattern of the bulk materials matched that generated from the single-crystal XRD study (see Supporting Information). IR (Nujol, $cm^{-1}$): 1615 (m), 1246 (m), 1211 (s), 1151 (m), 1115 (m), 1020 (m), 979 (w), 957 (w), 908 (w), 883 (m), 859 (m), 846 (w), 837 (m), 815 (w), 773 (w), 722 (w), 661 (w), 634 (w), 618 (w), 605 (m), 583 (m), 552 (w), 520 (w), 513 (w), 495 (w), 486 (w), 477 (w), 470 (w), 457 (w), 415 (m). Anal. Calcd for $Ti(\mu_{1,7}\text{-}OC_{10}H_6O)(\mu_{1,7}\text{:}\eta_2,\eta_1\text{-}OC_{10}H_6OH)(O^iPr)$ (found): C, 65.11 (65.05); H, 4.72 (4.71); N, 0.00 (<0.02).

**Single-Crystal X-ray Structure Determinations. 6. $[Ti_2(\mu_{1,4}\text{-}OC_6H_4O)_2(\mu_{1,4}\text{-}OC_6H_4OH)_2(\mu\text{-}OC_6H_4OH)_2]_\infty$ (2).** Crystals were grown from ether as explained in the text. A few milligrams of crystals were suspended in paratone oil on a glass slide. Handling the crystals in paratone for a few hours in the ambient atmosphere caused no apparent decomposition. Under a microscope, a single parallelogram-shaped crystal was isolated in a rayon fiber loop epoxied to a glass fiber.[61,62] On the F2 line at CHESS, the crystal was frozen in a 110 K nitrogen stream. Crystal to detector distance was set as small as possible (30 mm) because of the anticipated small unit cell size. A 2048 × 2048 pixel charge-coupled device was used to record the diffraction.[62,63] Data were collected as 5 min, 10° oscillations, with a total of 200° collected. The first frame was indexed using the program DENZO;[64] the remaining frames were also indexed with DENZO, and all the data was scaled together with SCALEPACK. The structure was solved by direct methods (SHELXS). Hydrogen atoms were introduced geometrically. The structure was refined by full-matrix least-squares on $F^2$ (SHELX-93) using anisotropic thermal parameters for all non-hydrogen atoms.

**2. $[Ti_2(\mu_{1,4}\text{-}OC_6H_4O)_2(\mu_{1,4}\text{:}\eta^2,\eta^1\text{-}OC_6H_4O)_2(OH_2)_2\cdot(H_2O)_2\cdot(HOC_6H_4OH)\cdot(Me\text{-}CN)]_\infty$ (4).** Crystals were grown from acetonitrile as explained in the text. A few milligrams of crystals were suspended in paratone oil on a glass slide. Handling the crystals in paratone for a few hours in the ambient atmosphere caused no apparent decomposition. Under a microscope, a single hexagon-shaped crystal was isolated in a rayon fiber loop epoxied to a glass fiber.[61,62] On the F2 line at CHESS, the crystal was frozen in a 113 K nitrogen stream. Crystal to detector distance was set at 30 mm. A 2048 × 2048 pixel charge-coupled device was used to record the diffraction.[62,63] Data were collected as 5 min, 10° oscillations, with a total of 200° collected. The first frame was indexed using the program DENZO;[64] the remaining frames were also indexed with DENZO, and all the data was scaled together with SCALEPACK. The structure was solved by direct methods (SHELXS). Hydrogen atoms were introduced geometrically. The structure was refined by full-matrix least-squares on $F^2$ (SHELX-93) using anisotropic thermal parameters for all non-hydrogen atoms.

**8. $[Ti_2(\mu_{1,7}\text{-}OC_{10}H_6O)_2(\mu_{1,7}\text{:}\eta^2,\eta^1\text{-}OC_{10}H_6OH)_2(O^iPr)_2]_\infty$ (5).** Crystals were obtained as described above. A dusting of crystals was placed in Paratone oil on a glass slide. Using a microscope, a single crystal was isolated in a 0.1 mm rayon fiber loop mounted with epoxy on a glass fiber.[61,62] On the A1 line at CHESS, the crystal and Paratone oil in the loop were frozen in a 108 K nitrogen stream. The crystal to detector distance was set at 38 mm. A 2048 × 2048 pixel charge-coupled device operating in a binned mode[62,63] was used to record the diffraction. Data were collected with 5 s, 2° oscillations for a total of 360°. The data frames were corrected for background and indexed sequentially using DENZO.[64] All the data was corrected for Lorentz and polarization effects, and scaled together with SCALEPACK. The structure solution was obtained by direct methods (SHELXTL). Hydrogen atoms were introduced geometrically. The structure was refined by full-matrix least squares on $F^2$ using isotropic thermal parameters for all non-hydrogen atoms except Ti, which was refined anisotropically.

**Acknowledgment.** We gratefully acknowledge contributions from the National Science Foundation (CHE-9528914, Inorganic Materials Traineeship to T.P.V. (DMR-9256824), Cornell High Energy Synchrotron Source (CHESS), Cornell Center for Materials Research (DMR-9632275); MSC REU to J.P.), and Cornell University.

**Supporting Information Available:** X-ray structural data pertaining to $[Ti_2(\mu_{1,4}\text{-}OC_6H_4O)_2(\mu_{1,4}\text{:}\eta^2,\eta^1\text{-}OC_6H_4O)_2(OH_2)_2\cdot(H_2O)_2\cdot(HOC_6H_4OH)\cdot(MeCN)]_\infty$ (**4**) and $[Ti_2(\mu_{1,7}\text{-}OC_{10}H_6O)_2(\mu_{1,7}\text{:}\eta^2,\eta^1\text{-}OC_{10}H_6OH)_2(O^iPr)_2]_\infty$ (**5**): a summary of crystallographic parameters, atomic coordinates, bond distances and angles, and anisotropic thermal parameters; and observed and calculated powder XRD for **2**, **4**, and **5**. The X-ray structural information pertaining to $[Ti_2(\mu_{1,4}\text{-}OC_6H_4O)_2(\mu_{1,4}\text{-}OC_6H_4OH)_2(\mu\text{-}OC_6H_4OH)_2]_\infty$ (**2**) may be found as Supporting Information to ref 56. This material is available free of charge via the Internet at http://pubs.acs.org.

IC990109B

(61) Blond, L.; Pares, S.; Kahn, R. *J. Appl. Crystallogr.* **1995**, *28*, 653−654.

(62) A throrough explanation of the construction of fiber loops and experimental methods at CHESS is given in: Walter, R. L. Ph.D. Thesis, Cornell University, 1996.

(63) (a) Thiel, D. J.; Walter, R. L.; Ealick, S. E.; Bilderback, D. H.; Tate, M. W.; Gruner, S. M.; Eikenberry, E. F. *Rev. Sci. Instrum.* **1995**, *3*, 835−844. (b) Walter, R. L.; Thiel, D. J.; Barna, S. L.; Tate, M. W.; Wall, M. E.; Eikenberry, E. F.; Gruner, S. M.; Ealick, S. E. *Structure* **1995**, *3*, 835−844.

(64) Otwinski, Z. *DENZO: a program for automatic evaluation of film densities*; Department for Molecular Biophysics and Biochemistry, Yale University: New Haven, CT, 1988.